In-situ neutron diffraction study on the tension-compression fatigue behavior of a twinning induced plasticity steel

Q. Xie[1], J. Liang[2], A. D. Stoica[1], R. Li[3], P. Yang[3], Z. Zhao[2], J. Wang[4], H. Lan[5], R. Li[4], K. An[1,*]

1. Chemical and Engineering Materials Division, Oak Ridge National Laboratory, Oak Ridge, TN 37831, USA
2. Collaborative Innovation Center of Steel Technology, University of Science and Technology Beijing, Beijing 100083, China.
3. School of Materials Science and Engineering, University of Science and Technology Beijing, Beijing 100083, China
4. State Key Laboratory for Advanced Metals and Materials (SKLAMM), University of Science and Technology Beijing, Beijing 100083, China
5. School of Electronics and Information, Jiangsu University of Science and Technology, Jiangsu 212003, China

Abstract

Evolution of the peak intensity for different grain orientations was in-situ measured by neutron diffraction for a twinning induced plasticity steel during tension-compression fatigue tests. Amplitude of the intensity variation is larger in high cycles than that at early cycles. The hysteresis loop features an asymmetric shape at early cycles and becomes symmetric with increase of cycles. Different twinning/detwinning activities correspond to different shape of the hysteresis loop. In cycle one, limited fresh twin volume is expected to correspond to short period of detwinning/retwinning. At later cycles, the twinning and detwinning are expected to happen together throughout the whole cycle.

Keywords

Twinning, detwinning, retwinning, fatigue, neutron diffraction

The twinning induced plasticity (TWIP) steel features a remarkable combination of ductility and strength [1]. Deformation twinning was identified being the main deformation mechanism in the TWIP steel [2] and crucial for its mechanical performance, which was also found playing a dominant role at the initial stage of plasticity [3]. The loading modes, temperature, residual strain, grain size, stacking fault [4], grain orientation [5] and strain rate, all can influence the activation of deformation twinning [6, 7]. The twinning behavior becomes more complex during cyclic loadings than monotonic loadings, as in the cyclic loadings both detwinning (the same twin variant as that in previous twinning) and retwinning (different twin variant from that in previous twinning) could be introduced because of the change

*corresponding author: *Ke An* kean@ornl.gov.

of the loading direction (LD). The mechanical behavior of the TWIP steel can be nicely repeated by combining the ab initio and a constitutive model based on the substructure [8, 9, 10]. During the complex loading, in-situ characterization tools have advantage in revealing the dynamic behavior [11]. Engineering neutron diffraction has the advantage to measure the twinning micromechanical behavior in-situ which is ascribed to its capability of high penetration power [12] and sensitivities to the diffraction intensity changes of crystallographic orientations [11]. In this paper, we studied the fatigue behavior in a TWIP steel where concomitant grain orientation density change was detected.

The chemical composition of the studied material is 0.57% C, 17.74% Mn, 2.96% Si, 0.44Al, Bal. Fe (weight percent). The as-received plate was after forging (forging started at ~1050 °C and finished at ~750°C). Cylindrical dog-bone samples were cut using the electrical discharge machining followed by mechanical machining. They were then annealed at 450°C for 1 hour in vacuum to remove the residual strain. The gauge section is Φ 6.35 mm × 20 mm. The sample was first loaded to 0.8% engineering strain and then experienced 0.125 Hz fully reversed cyclic loading with ±0.8% engineering strain amplitudes. During the neutron diffraction measurement, the strain control was slowed down to one hour/cycle to get good neutron-data statistics. The geometrical setup of the in-situ neutron measurement was given in supplementary material. Electron backscatter diffraction (EBSD) was performed with 20 kV with a step size of 0.3 μm in the electron microscope. At certain deformation zone, small step size of 0.05 μm was used. The EBSD samples were processed by electrolytic polishing using 20% perchlorate acid solution in alcohol (voltage 15 V for 25 seconds).

The initial microstructure is shown in Fig.1a. The diffraction pattern along the axial direction shows a single-phase material with face centered cubic (FCC) structure. The refined initial texture index is ~1 meaning a random texture. During the cycles, the change of the detected peak intensity was observed as shown by the example in the 1000^{th} cycle in Fig. 1c. The corresponding variation of the texture index within one cycle ranged from 1.01 to 1.19.

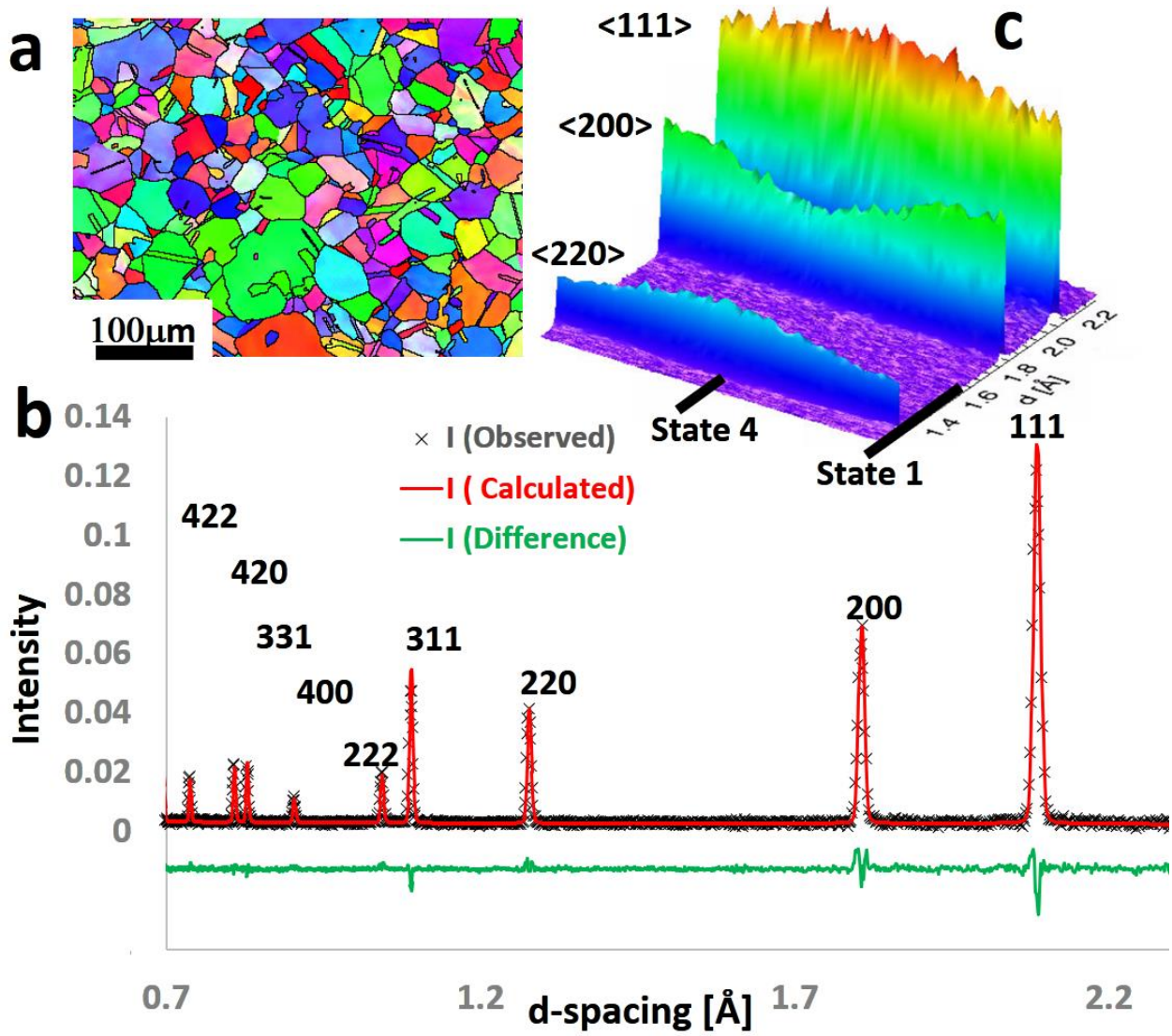

Figure 1 The microstructure of as-received sample of the studied TWIP steel (a) and the corresponding neutron diffraction pattern (b). Obvious orientation density change during cycle 1000 were observed as given in (c).

The representative stress-strain curves of the selected cycles are given in Fig.2a. Asymmetric hysteresis loading loops were profound in the early cycles and they gradually became symmetric and stable after 100 cycles. The hysteresis loop is different from that reported in [13] which did not show the asymmetric behaviors due to twinning. The twinning behavior in our sample is expected more than that in [13]. The grain size in the current sample is more than ten times larger than theirs (~7 μm reported in [13]). The twinning was found active at the start of the plastic deformation with large grain size (~85μm) [14], and the deformation twins can be found during cyclic loadings with stress amplitude even lower than the yield stress [15] and in high cycles of fatigue test [16]. The grain size, chemical composition and

the stacking fault can give a non-linear deviation in the twinning among different TWIP steels [17]. The unloading curve after tension of the TWIP steel was found nonlinear [18] as similarly shown in our tests. The cause of nonlinear unloading could be related to detwinning. Since twinning/detwinning can induce abrupt grain orientation change which is different from the dislocation slip, in-situ neutron diffraction can provide evidences of this behavior with appropriate detector coverage. The VULCAN instrument utilizes the area detectors and its angular coverage is sufficient to study the orientation change using neutron diffraction for cubic metals. Fig.S1b in supplementary material gives the covering area in the inverse pole figure (IPF) for different peak detected on VULCAN.

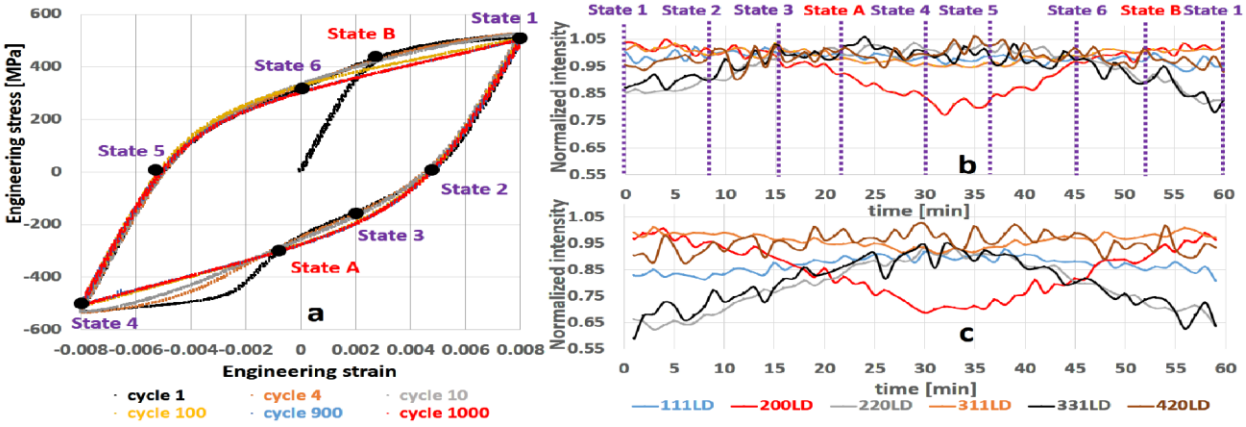

Figure 2 The representative engineering stress as a function of engineering strain for cycle 1, 4, 10, 100, 900, 1000, including the initial tensile loading of the test (a). Evolution of the integrated peak intensities (normalized by the corresponding intensities before the start of the fatigue loading) measured by neutron diffraction along LD as a function of time for cycle 1 (b) and cycle 1000 (c). Certain key states were marked and they were also marked in a.

Orientation dependent twinning behavior has been studied [17, 19-22]. The appearance of twinning was found complying with the Schmid law at small strain [17]. In tension, twinning was observed in a wide range of orientations: mainly in <1 1 1> and <1 1 0> orientations but no twinning was observed in <1 0 0> orientations [17, 19-21]. In compression <100> grains mainly experienced twinning behavior [22]. Fig.2b and c give the evolution of the integrated peak intensities in Cycle 1 and Cycle 1000, respectively. Change of peak intensity of the slip dominant grains (<311> and <420> peaks) is smaller than that of the twinning favoring ones (<331>, <002> and <220> peaks). The change of intensity of the <111> peak is small although it is favoring twinning in tension. Note that the intensity of the <111> peak is increasing in tension and decreasing in compression due to dislocation slips. However, for the measured <111> peak intensity, it is slightly decreasing in tension and increasing in compression. This suggests the dominant role of

twinning/detwinning in grains with <111>//LD. While otherwise considering slips as the dominant one, there is too much discrepancy in both macroscopic deformation and evolution of the peak intensity as shown in Fig.S2. Therefore, one can conclude that the twinning, retwinning/detwinning behaviors were dominant and ascribed to the big change of the orientation density as evidenced by the in-situ neuron diffraction data.

In Fig.2, state 1 and 4 are at maximum tensile and compressive loads, respectively. State 2 and 5 are at zero macroscopic load after unloading of tension and compression, respectively. State 6 and 3 are at zero macroscopic strain during tension and compression, respectively. Two intermediate state A and B are introduced for Cycle 1. For the <331> and <220> peak intensities, they changed relatively small in Cycle 1 between state 3 and 4 (detwinning is expected). The <200> peak intensity changed small between state 6 and 1 (detwinning is expected[†]). For both cases, they should be due to limited twin volume since certain level of pre-strain is necessary for nucleation of the deformation twin [23]. Then the detwinning/retwinning finished at the intermediate state A and B. Indeed, the change of the intensity amplitude in cycle 1 is smaller than in cycle 1000. Accurate twin volume fraction can be measured using the electron channeling contrast imaging (ECCI) technique [4, 8, 9, 10]. In neutron diffraction, the integrated peak intensity of certain peak is proportional to the number of unit cells that are preferentially oriented to fulfill Bragg's law within the scattering volume [24]. One can estimate the average twin volume variation from the change of the peak intensity. The variation of the <220> peak is increased ~100% from cycle 1 to cycle 1000 and this means that the involved twin volume fraction is doubled at the end of the 1000th cycle. In Cycle 1000, the twinning-detwinning behavior for the <331>, <220> and <200> grains seem to occur almost in the whole cycle. Note also that from state 1 to A and roughly from state 4 to B, the trend of peak intensity evolution in Cycle 1 and 1000 are similar, the corresponding loading curves are also similar. For the rest, they are different in the trend of the peak intensity evolution. There is not yet a model to treat the twinning/detwinning behavior to calculate the corresponding flow stress curves, which takes into account both the local stress heterogeneity due to twinning and the interaction of multiple twin systems. The dislocation configurations after twinning/detwinning [25] were not considered in the popular crystal plasticity models, although the dislocation dynamic is the physical basis of the crystal plasticity models. Current results are helpful for validation of the twinning models.

Deformation twins were also evidenced from the EBSD observation. Fig.3 gives one typical deformation morphology after Cycle 1000. The EBSD image quality

[†] From state A to state 4, twinning in the <13,1,1> grains are expected to occur together with twinning in the <200> grains. The former can induce the increase in intensity of the <331> peak. However, the increase of the <331> peak at this stage is limited. This is related to the detection possibility as explained in supplementary material.

(IQ) map was often used to show the deformation twins [26]. The orientation relationship between the matrix and the twin was identified being ~70.5˚ rotation about <110> axis which corresponds to a minimum misorientation of ~60˚ rotation around <111> axis. The two banded structures were identified along the {111} plane and are corresponding to the largest and the second largest Schmid factors of the twinning systems. This satisfies the type III structure mentioned in [9].

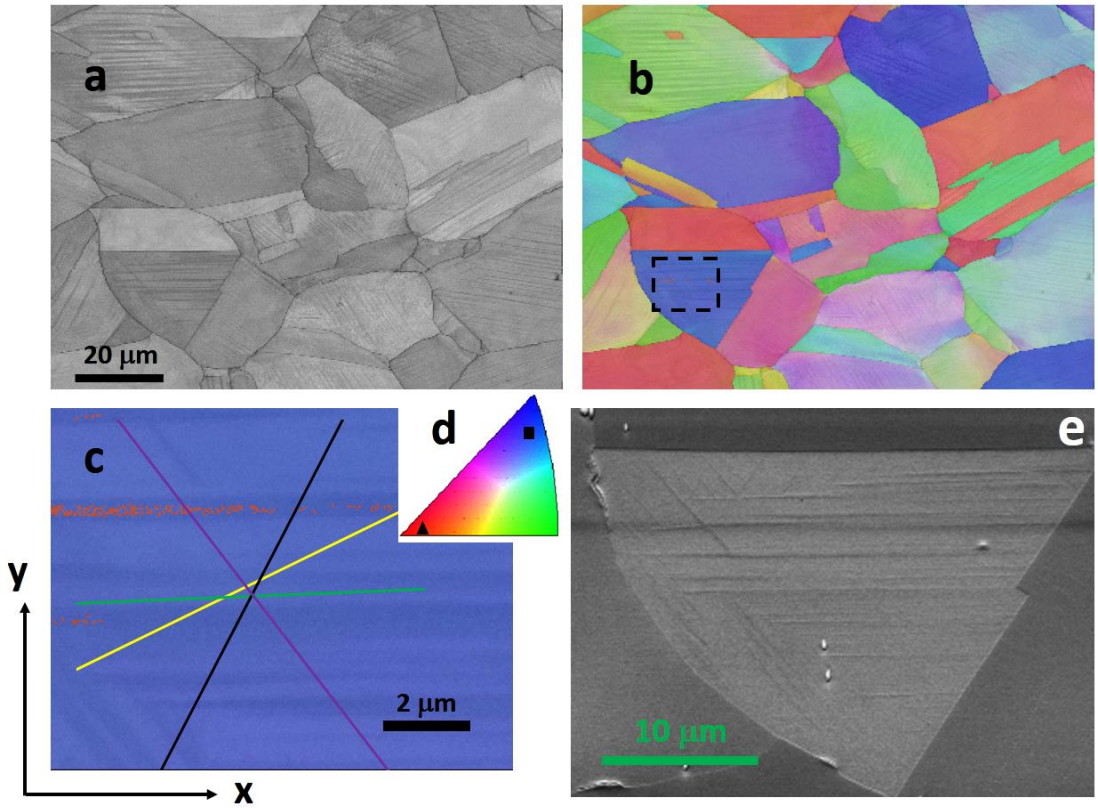

Figure 3 Microstructure observed by EBSD measurement. The image quality map is in (a), the grain orientation contrast is given in (b) and the magnification of the inset is given in (c) and the color IPF triangle is in (d). The detected matrix orientation ■ and the twin orientation ▲are marked in (d). The corresponding SEM image of (d) is in (e). The {111} plane trace is marked in (c) and the Schmid factor of the involved twin systems are given in supplementary material.

Like the magnesium alloys under cyclic loadings [27], it is necessary to clarify whether or not the twins formed during the tensile loading could retwin or detwin, or only dislocation slips occur in the subsequent compression and vice versa. The triangle of the loading direction inverse pole figure (LDIPF) can be divided into the twin favoring zone and slip favoring zone in tension and compression respectively as given in Fig.4. The twin favoring zones can be divided into two zones if the new orientation favors (1) the twinning or (2) the dislocation slips once the LD reverses.

The former can be further divided as (1) twining-detwinning dominant zone if the new twin variant is the same as the previous one or (2) twinning-retwinning zone if the new twin variant is different from the previous one.

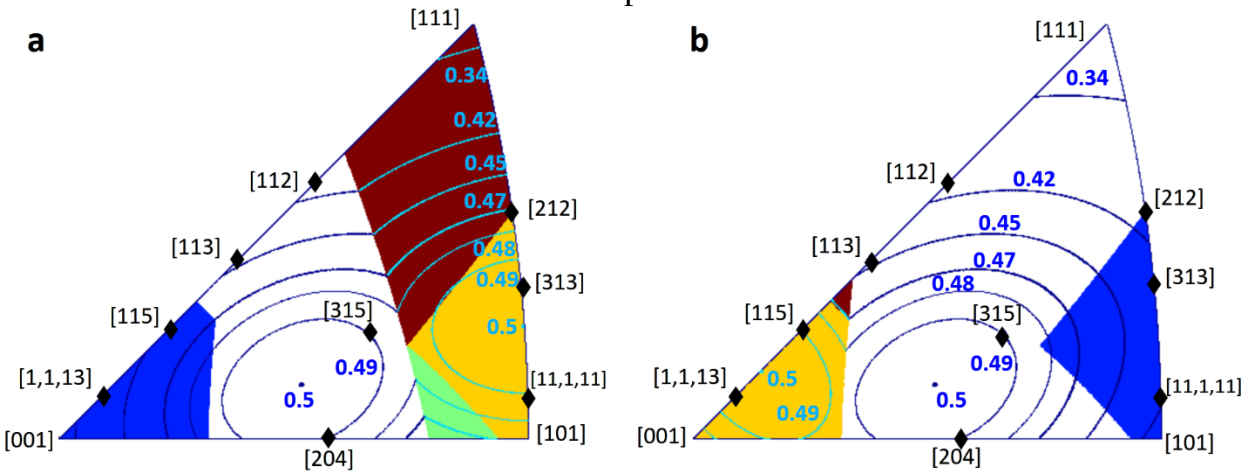

Figure 4 Schmid factor distribution for twinning and slip during tensile (a) or compression (b) phase of the fatigue loading. In the twin active zones, twining followed by detwinning (yellow), or retwinning (brown), or dislocation slip (green) were identified. The blue area indicates the region of the new orientation after twinning for grains in the yellow area.

Multiple slip systems activation is also considered in Fig.4. For grains with <111>//LD, there are three variants of twin active in tension. For any of them, the new orientation will be <511>//LD. In the subsequent compression, the twin will rotate to <11,11,1>//LD. The new twin will undergo twin-detwin between orientations <511>//LD and <11,1,11>//LD afterwards. We call the behavior in the first cycle twinning-retwinning because of the change of the twin variant and this is different from the twinning-detwinning. This is true for all grains with orientations marked by the brown color in Fig.4. The above analysis only considers the deformation geometry due to twinning. Note that twin variants with the second and the third largest Schmid factors are neglected so far. Fig.4 cannot explain the slightly increase in compression for the <111> peak since once the <111> grain twins to the <511> orientation, the twins cannot twin back to the <111> orientation in compression. However, for grains with <511>//LD, the twins with the second largest Schmid factor can twin to the <111> orientation in compression.

Due to the existence of different zones in Fig.4, the micromechanical behavior in fatigue loading is complex. (a) the new orientation after twinning is always in the dislocation slip favoring zone during either tension or compression. Therefore, there is strong interaction between the narrow twin boundary and the dislocation slip in the thin twin plates [21, 22]. (b) The new orientation zone after twinning during tension is in the twinning favoring zone for compression, and vice versa. Therefore,

the detwinning/retwinning could easily happen during the tension-compression type of cyclic loading. (c) In compression, decrease of the <200> peak can be due to twinning of twins in the <200> matrix or due to detwinning of twins in the <221> matrix. In tension, increase of the <200> peak intensity can be due to detwinning of twins in the <200> matrix or due to twinning of twins in the <221> matrix. Similar analysis is applied to grains with <331> or <220>//LD. (d) The co-existence of twinning, retwinning, detwinning and dislocation slips during the tension and compression makes the analysis on the micromechanical behavior in fatigue loading complex.

We found that the <331> and <220> grains feature the compressive lattice strains at state 2 after macroscopic unloading. The compressive stress at state 2 promotes the detwinning in these grains. This results a load redistribution among different grains and consequently the macroscopic unloading curve is slightly nonlinear. This is similar to the nonlinear type of unloading in magnesium alloy [28].

In summary, we demonstrated the in-situ neutron diffraction measurements on the fatigue behavior of a TWIP steel. The hysteresis loop features an asymmetric shape at early cycles and becomes more symmetric with increase of cycles. In the first cycle, limited fresh twin volume corresponds to short period of detwinning/retwinning behavior for grains with the <220> or <331>//LD during compression and that for grains with the <200>// LD in tension. The detwinning at unloading induces a non-linear type of macroscopically unloading curve due to the load re-distribution. At later cycles, the twinning and detwinning happened together almost throughout the whole cycle and even at very small applied stress levels. This agrees with the fact that the area of the loop in early cycles is larger than the stable ones (after 100 cycles). The change of the area mainly happens at the stage where twinning is dominant in early cycles, which was later replaced by easier deformation of both twinning and detwinning.

Acknowledgements

Q. XIE thanks the funding from the Natural Science Foundation of China (grant no. 51571025) during his former post-doc period at the University of Science and Technology Beijing. Q. XIE also thanks the support of a Laboratory Directed Research and Development project at the Oak Ridge National Laboratory. Neutron work was done at the Spallation Neutron Source, a DOE Office of Science User Facility operated by the Oak Ridge National Laboratory.

References

[1] A. S. Hamada, L. P. Karjalainen, J. Puustinen, Mat. Sci. Eng. A-Struct. 517(2009) 68–77.
[2] S. Vercammen , B. Blanpain, B.C. De Cooman, P. Wollants, Acta Mater. 52(2004) 2005–2012.
[3] Y. Li, L. Zhu, Y. Liu, Y. Wei, Y. Wu, D. Tang, Z. Mi, J. Mech. Phys. Solids 61(2013) 2588–2604.
[4] I. Gutierrez-Urrutia, D. Raabe, Scr. Mater. 69 (2013) 53-56.
[5] D.T. Pierce, J. A. Jiménez, J. Bentley, D. Raabe, J.E. Wittig, Acta Mater. 100 (2015) 178-190.
[6] B. C. De Cooman, O. Kwon, K. G. Chin, Mater. Sci. Tech. SER, 28(2012) 513-527.
[7] J.W. Christian and S. Mahajan, Prog. Mater. Sci. 39(1995) 1-157.
[8] D. R. Steinmetz, T. Jäpel, B. Wietbrock, P. Eisenlohr, I. Gutierrez-Urrutia, A. Saeed–Akbari, T. Hickel, F. Roters, D. Raabe, Acta Mater. 61(2013) 494-510.
[9] D. Raabe, F. Roters, J. Neugebauer, I. Gutierrez-Urrutia, T. Hickel, W. Bleck , J. M. Schneider , J. E. Wittig and J. Mayer, 41 (2016) MRS Bull. 320-325.
[10] I. Gutierrez-Urrutia, D. Raabe, Acta Mater. 59 (2011) 6449-6462.
[11] W. Wu, Y. F. Gao, N. Li, C.M. Parish, W. Liu, P.K. Liaw, K. An, Acta Mater. 121(2016) 15–23.
[12] Introduction to the Characterization of Residual Stress by Neutron Diffraction M.T. Hutchings, P.J. Withers, T.M. Holden, Torben Lorentzen, CRC Press; 2005.
[13] A. A. Saleh, E. V. Pereloma, B. Clausen, D. W. Brown, C. N. Tomé, A. A. Gazder, Acta Mater. 61(2013) 5247-5262.
[14] K.M. Rahman, V.A. Vorontsov, D. Dye, Acta Mater. 89(2015) 247–257.
[15] X. Wang, Z. Y. Liang, R. D. Liu, M. X. Huang, Mat. Sci. Eng. A-Struct. 647 (2015) 249–255.
[16] J. J. Roa, G. Fargas, J. Calvo, E. Jiménez-Piqué, A. Mateo, Mat. Sci. Eng. A-Struct. 628 (2015) 410–418.
[17] I. Gutierrez-Urrutia, S. Zaefferer, D. Raabe, Mat. Sci. Eng. A-Struct. 527 (2010) 3552-3560.
[18] E. J. Pavlina, M.G. Lee, F. Barlat, Metall. Mater. Trans. A. 46(2015) 18–22.
[19] H. Beladi, I. B. Timokhina, Y. Estrin, J. Kim, B.C. De Cooman, S.K. Kim, Acta Mater. 59(2011) 7787-7799.
[20] D. Geissler, J. Freudenberger, A. Kauffmann, M. Krautz, H. Klauss, A.Voss, J. Eickemeyer, L. Schultz, Acta Mater. 59 (2011) 7711–7723
[21] P. Yang, Q. Xie, L. Meng, H. Ding, Z. Tang. Scr. Mater. 55(2006) 629–631.
[22] L. Meng, P. Yang, Q. Xie, H. Ding, Z. Tang. Scr. Mater. 56(2007) 931-934.
[23] H. Qiao, M.R. Barnett, P. D. Wu, Int. J. Plasticity 86(2016) 70-92.

[24] W. Woo, H. Choo, D. W. Brown, Z. Feng, P. K. Liaw, S. A. David, C. R. Hubbard and M.A.M. Bourke (May 16-25, 2005), In S. A. David, T. Debroy, J. C. Lippold, H. B. Smartt. Trends in Welding Research: Proceedings of the 7th International Conference, Callaway Gardens Resort, Pine mountain, Georgia USA, 393-400.
[25] M. J. Szczerba, S. Kopacz, M.S. Szczerba, Acta Mater. 102(2016)162-168.
[26] K. Renard, H. Idrissi, D. Schryvers, P. J. Jacques, Scr. Mater. 66 (2012) 966–971.
[27] Q. Yu, J. Zhang, Y. Jiang, Philos. Mag. Lett. 91(2011) 757-765.
[28] L. Wu, S. R. Agnew, D. W. Brown, G. M. Stoica, B. Clausen, A. Jain, D. E. Fielden, P. K. Liaw, Acta Mater. 56(2008) 3699–3707.